Supplemental Data. Leivar et al. (2009). Definition of early transcriptional circuitry involved in light-induced reversal of PIF (phytochrome-interacting bHLH factor)-imposed repression of photomorphogenesis in young Arabidopsis seedlings.

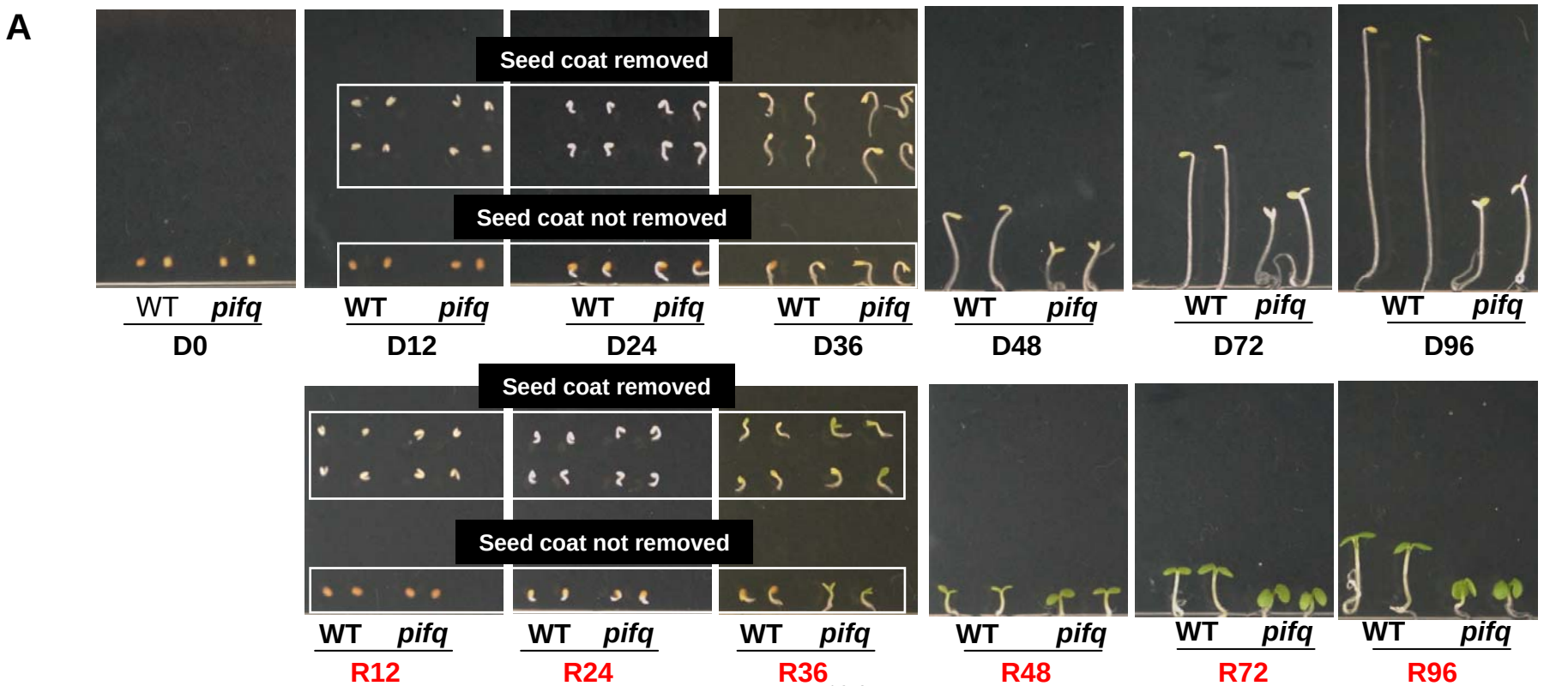

Supplemental Figure 1

<u>Supplemental Figure 1.</u> Complete time-course analysis of morphological phenotypes of *pifq* mutant seedlings grown in the dark and in Rc.

An extended time-course analysis was done in WT and *pifq* mutant seedlings. Seedlings were grown in darkness and in Rc for 12 to 96 h (D12-D96 and R12-R96) as in Figure 1A, except that 1.9 μmol/m^2/s of R was used.

A) Visible morphological phenotypes. Photos of representative WT and *pifq* mutant seedlings at the indicated time points are shown. Seedlings taken at 12, 24 and 36 h were also photographed after removing the seed coat.

B) Quantification of the cotyledon separation (left panel) and hypocotyl length (right panel) phenotypes. Data represent the mean and standard error of at least 20 seedlings.

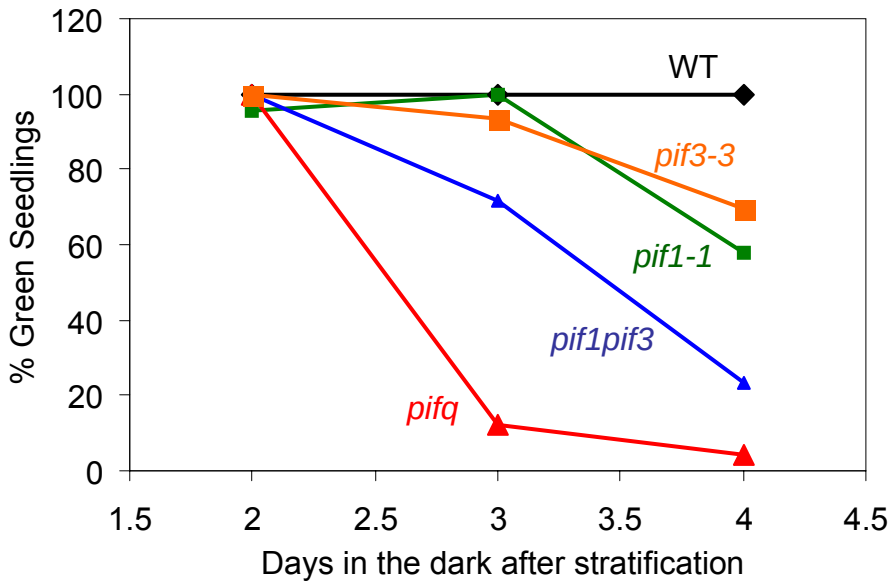

<u>Supplemental Figure 2.</u> Photobleaching phenotype of *pif1*, *pif3*, *pif1pif3* and *pifq* mutants grown under true-dark conditions before transfer to light.

Time-course analysis of the photobleaching phenotype in the indicated WT and *pif* mutant seedlings grown in darkness before transfer to WL, as in Figure 1D. The % of green seedlings was scored from at least 40 seedlings. *pif3* mutant corresponds to a batch of seeds that was grown independently from the rest. The *pif1pif3* double mutant was that previously described (Leivar et al., 2008b).

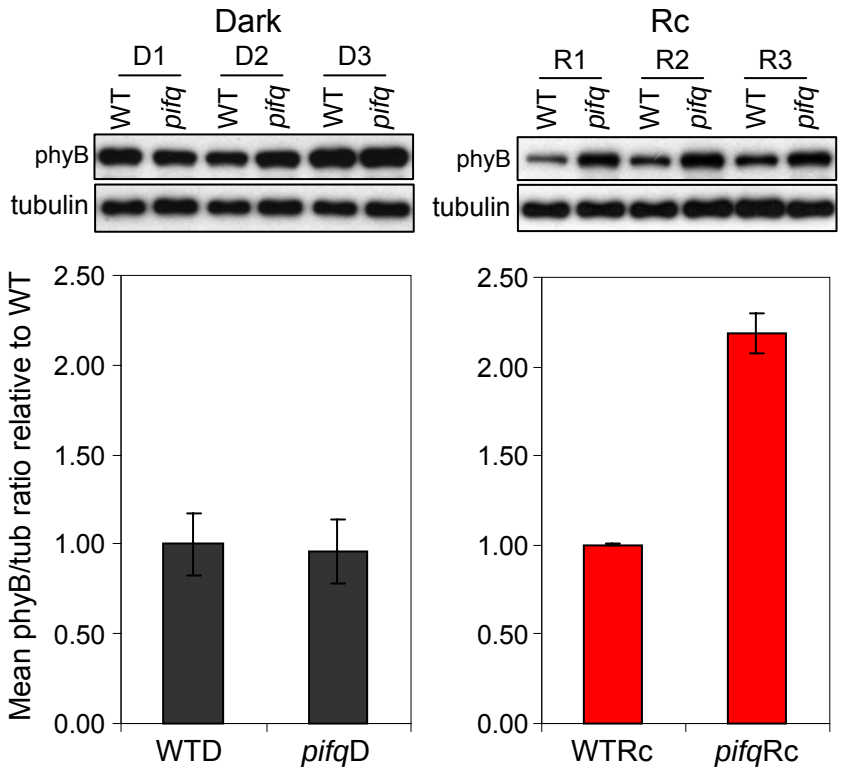

Supplemental Figure 3. Quantification of phyB levels in *pifq* mutant seedlings grown in the dark or in Rc for 2 days. Immunoblot analysis of phyB protein levels in WT and *pifq* mutant seedlings grown in the dark and in Rc (6.7 µmol/m^2/s) for 48h, as in Figure 1A. Protein extracts prepared from 3 biological replicates (labeled D or R1, 2 and 3) were immunoblotted with an anti-phyB antibody (top). One of the biological replicates is also shown in Figure 1G. Tubulin was used as loading control. phyB signal normalized to tubulin was quantified from the blots using Image J software as described (Leivar et al., 2008a). phy/tubulin ratio is represented as the mean and standard error of the 3 independent biological replicates (bottom), and the values are relative to the mean of WT-D (left panel) or WT-Rc (right panel).

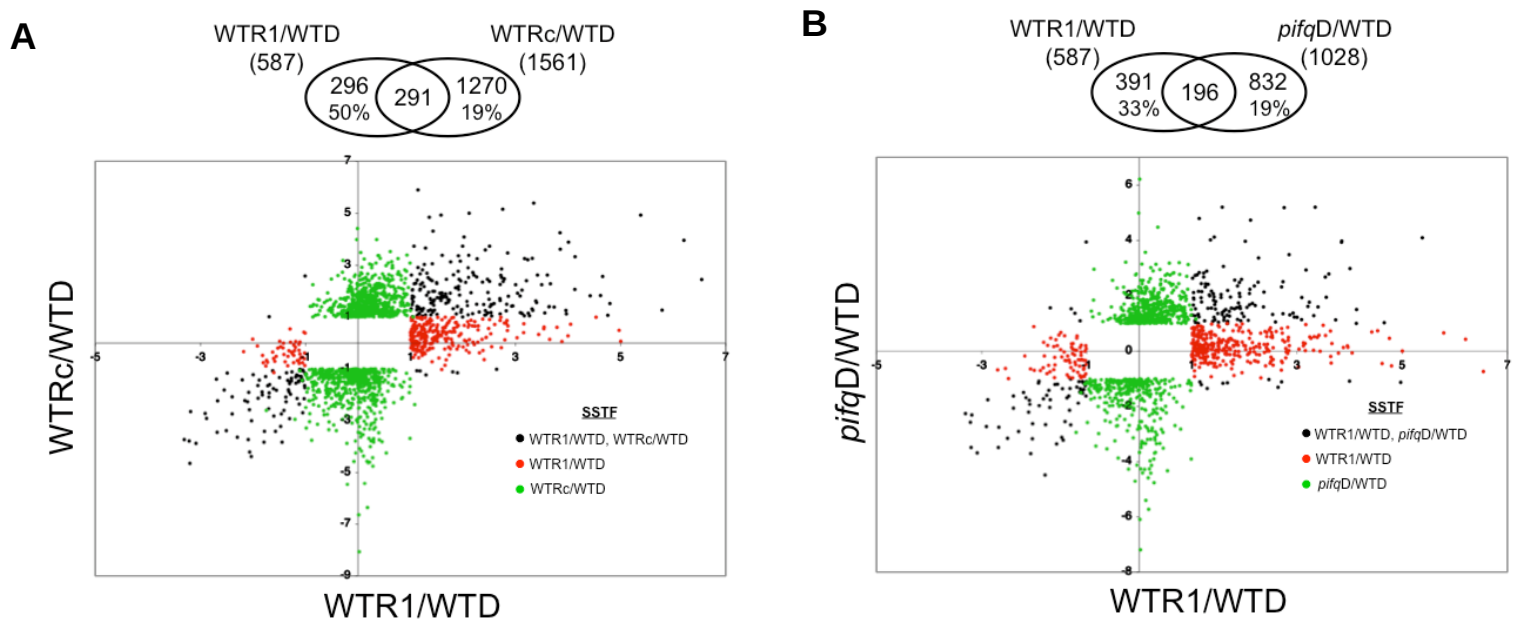

<u>Supplemental Figure 4.</u> Comparison of early R-responsive genes with long-term R-responsive genes and PIF-regulated genes in the dark.

Venn diagrams in panels A and B (top) show pairwise comparisons of the SSTF differentially-expressed genes for each genotype-growth-treatment combination. The number and percentage of shared genes in each comparison are indicated. Scatterplots of log2 fold-change values in panels A and B (bottom) provide a quantitative measure of the correlation in responsiveness for each gene between the genotype-growth-treatment combinations compared. Black dots in the scatterplot represent genes that are shared between the two combinations in the Venn diagram (top) whereas red and green dots represent genes that are specifically present in one of the combinations but not in the other.

A) Comparison of early (WT-D vs WT-R1) and long-term (WT-D vs WT-Rc) R-responsive genes in wild-type seedlings.

B) Comparison of early R-responsive (WT-D vs WT-R1) and PIF-regulated genes in dark-grown seedlings (WT-D vs *pifq*-D).

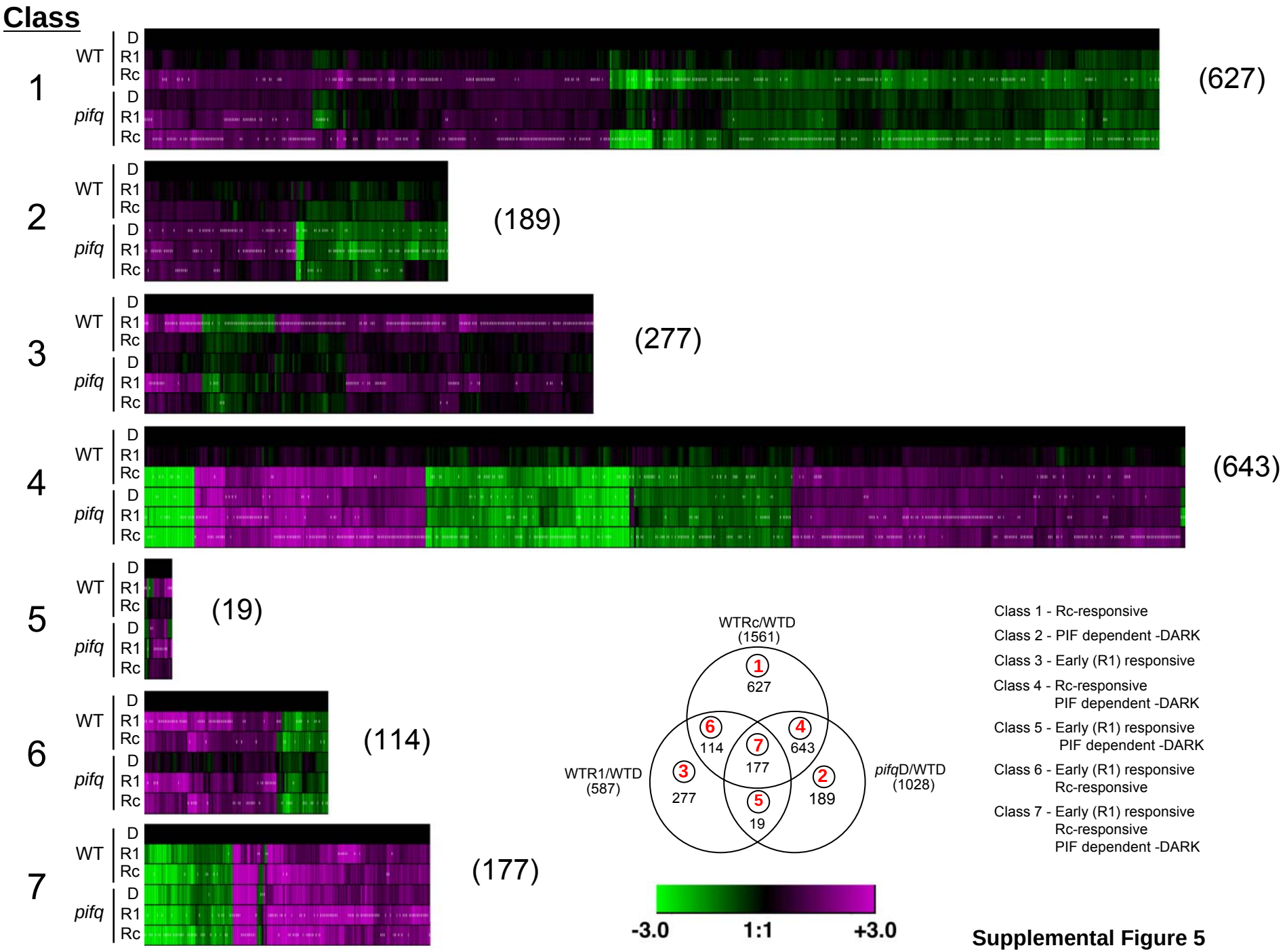

Supplemental Figure 5

Supplemental Figure 5. Hierarchical cluster analysis of Class 1-7 SSTF genes responding to WT-R1, WT-Rc and/or *pifq*-D reported in Figure 4A.

Hierarchical cluster analysis of the genes in Classes 1-7 (defined lower right, as in Figure 4A) was performed with Genesis software (Sturn et al., 2002). The numerical values for the green-to-magenta gradient bar (bottom) represent log2-fold change relative to WT–D. White dots indicate absolute maximum of expression change for each gene among the six genotype-treatment combination. The number of genes in each class is shown in parenthesis on the right side of the heat map.

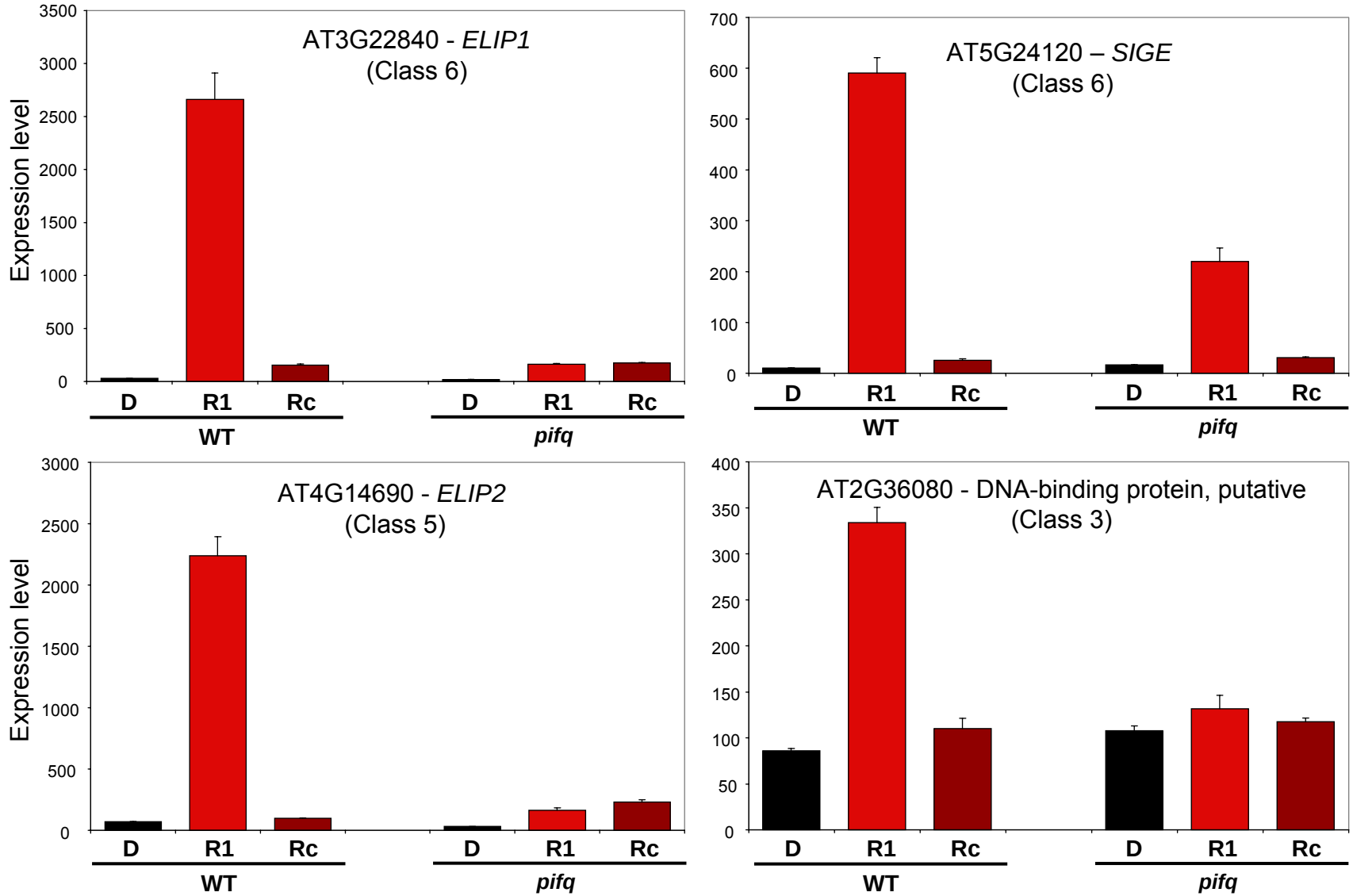

<u>Supplemental Figure 6.</u> Expression profiles of examples of early-R1 induced genes that are dependent on the PIFs for this R-light-induction.

The four examples provided represent expression patterns in the *pifq* mutant that are similar to the expression patterns reported in *pif3* monogenic mutants (Monte et al., 2004). Data represent mean expression and standard error of at least 3 biological replicates.

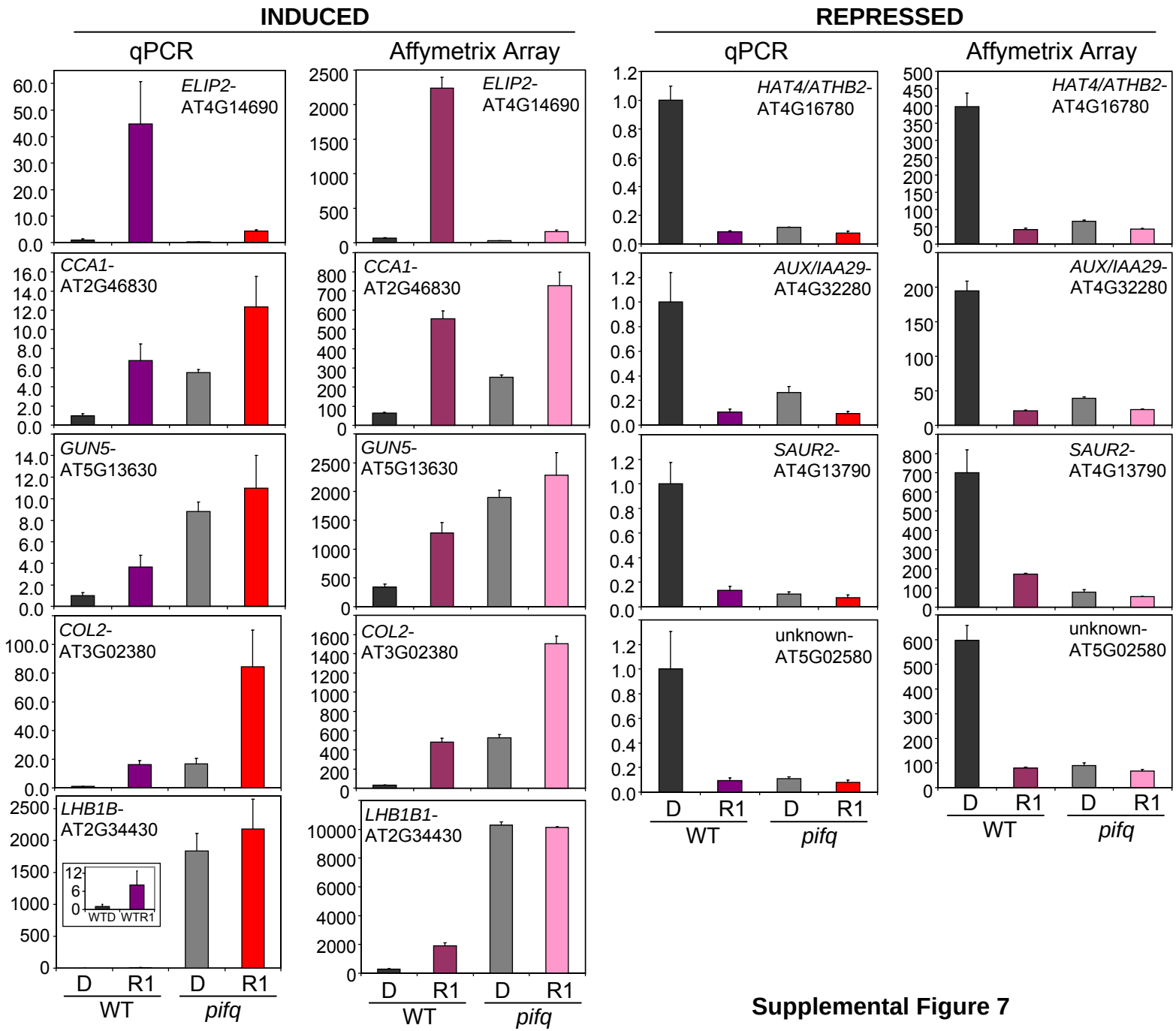

Supplemental Figure 7

Supplemental Figure 7. Q-PCR validation of the expression of selected early R1-responsive genes that are PIF-dependant in the dark.

The expression data obtained by q-PCR (Figure 6) on selected genes is compared to the expression data obtained by the Affymetrix array (Supplemental Dataset 1). WT and *pifq* mutant seedlings were grown as in Figure 3A. Expression data by q-PCR was normalized to PP2A and is presented relative to the mean of WT-D set at unity. Q-PCR data represent the mean and standard error of 3 independent biological replicates.

<u>Supplemental Figure 8</u>. Expression profiles of phy-PIF-regulated genes potentially involved in enhanced mobilization of oil bodies.

The expression patterns of the genes shown in panels A-C belong to Class 4 in Figure 4A (defined as responsive to both WT-Rc and *pifq*-D relative to WT-D). Data represent mean expression and standard error of at least 3 biological replicates.

A) Induced putative lipase genes.

B) Repressed glyoxysome marker gene.

C) Induced peroxisome marker gene.

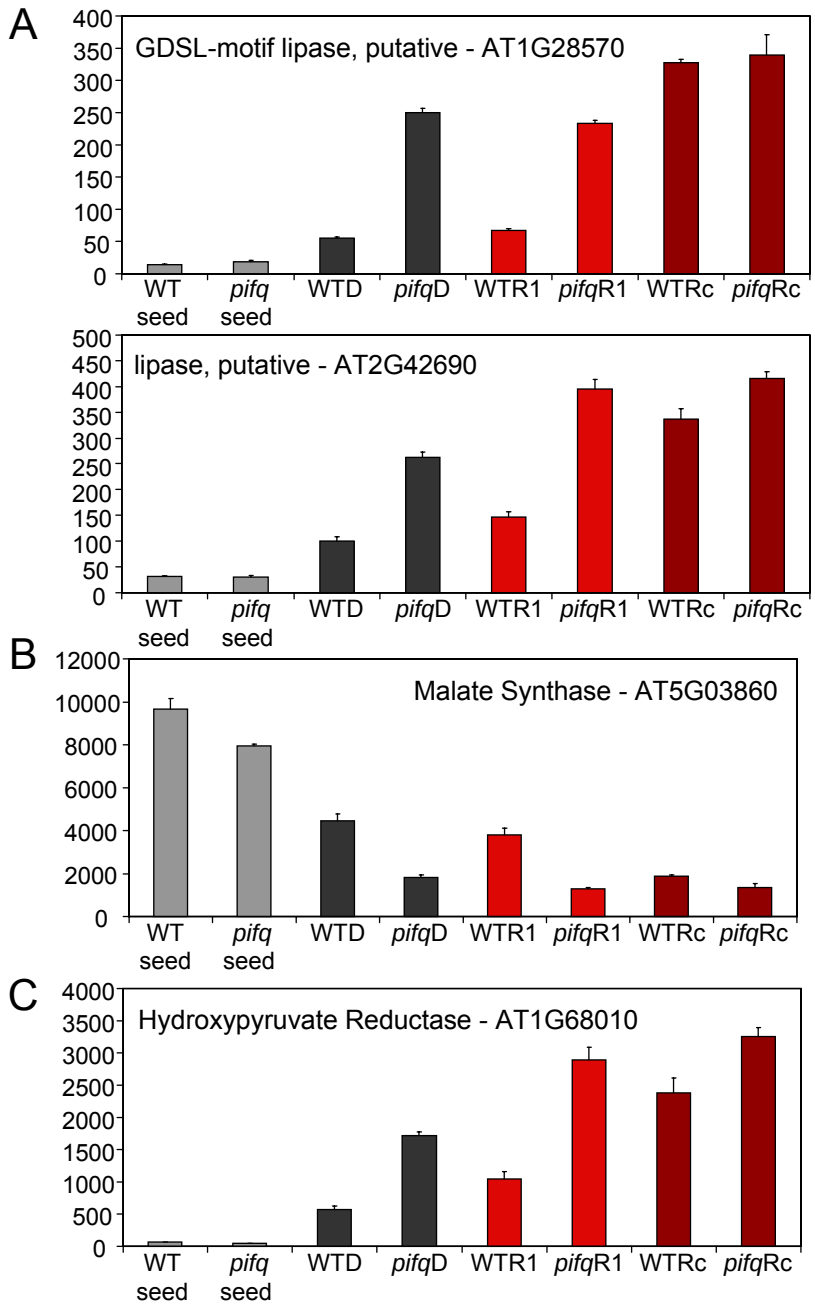

A

	WITH G-box	TOTAL	% with G-box
ATH1_Genes	7467	22153	33.7

B

Induced

	TOTAL	% WITH G-BOX	P VALUE
Class 1_induced	**287**	**39%**	**0.02476698**
Class 2_induced	95	41%	0.0808349
Class 3_induced	**232**	**53%**	**2.19E-09**
Class 4_induced	382	37%	0.1208429
Class 5_induced	**9**	**78%**	**0.008858728**
Class 6_induced	82	43%	0.05598833
Class 7_induced	**115**	**48%**	**0.001167494**

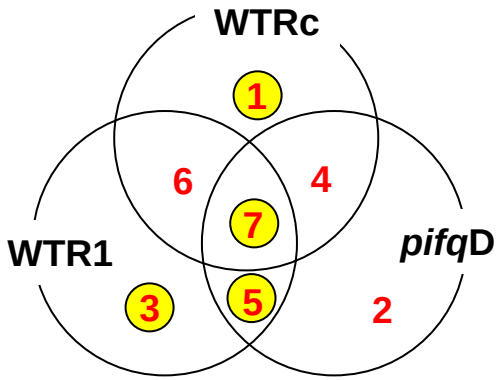

Repressed

	TOTAL	% WITH G-BOX	P VALUE
Class 1_repressed	340	37%	0.1044261
Class 2_repressed	94	39%	0.1463745
Class 3_repressed	**45**	**49%**	**0.02490749**
Class 4_repressed	**254**	**50%**	**2.64E-08**
Class 5_repressed	1	0%	1
Class 6_repressed	29	45%	0.1424631
Class 7_repressed	**56**	**59%**	**9.46E-05**

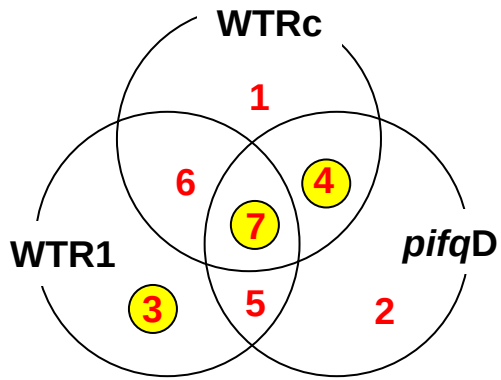

Supplemental Figure 9. Statistical analysis for G-box enrichment in the 3Kbp-upstream putative promoter regions of SSTF genes by Class.

A) Percent of genes represented on the ATH1 array with G-boxes in the 3-Kbp upstream sequence as determined using the Patmatch tool on the TAIR website (http://www.arabidopsis.org/cgi-bin/patmatch/nph-patmatch.pl).

B) Hypergeometric statistical test to asses the significance of G-box enrichment in the different SSTF genes by Class compared to the total population of genes represented on the ATH1 array (panel A). Induced and repressed genes Class 1-7 are described in Figure 4. Highlighted Classes in the Venn diagram (right panel) are the ones showing a statistically significant enrichment of genes with G-boxes (p-value ≤ 0.05).

A Induced

	TOTAL	% WITH G-BOX	P VALUE
PHOTOSYNTHESIS/CHLOROPLAST	**402**	**40%**	**0.004239335**
TRANSCRIPTION	**128**	**52%**	**2.27E-05**
HORMONE	17	29%	0.7295554
SIGNALING	61	44%	0.05566271
TRANSPORT	**52**	**50%**	**0.01098601**
STRESS/DEFENSE	57	35%	0.4618952
GROWTH/DEVELOPMENT	36	31%	0.713165
CELL METABOLISM	**270**	**40%**	**0.01721499**

Repressed

	TOTAL	% WITH G-BOX	P VALUE
PHOTOSYNTHESIS/CHLOROPLAST	**46**	**50%**	**0.01623301**
TRANSCRIPTION	**83**	**61%**	**2.10E-07**
HORMONE	29	28%	0.8131044
SIGNALING	37	43%	0.1461822
TRANSPORT	57	44%	0.07093162
STRESS/DEFENSE	**73**	**48%**	**0.008110258**
GROWTH/DEVELOPMENT	53	38%	0.3129517
CELL METABOLISM	244	36%	0.1965742

B Transcription-related genes by Class

Induced	WITH G-BOX	TOTAL	% WITH G-BOX	P VALUE
Class 1_induced	9	18	50%	0.1141109
Class 2_induced	3	6	50%	0.3269932
Class 3_induced	**30**	**50**	**60%**	**1.24E-04**
Class 4_induced	7	21	33%	0.5956202
Class 5_induced	1	2	50%	0.5605272
Class 6_induced	7	13	54%	0.1089621
Class 7_induced	9	18	50%	0.1141109
TOTAL INDUCED	**66**	**128**	**52%**	**2.27E-05**

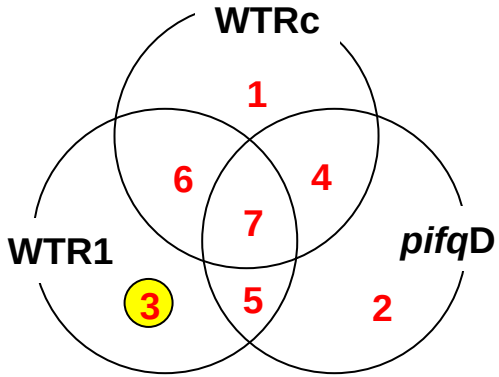

Repressed				
Class 1_repressed	**10**	**18**	**56%**	**0.04660887**
Class 2_repressed	3	8	38%	0.5409452
Class 3_repressed	8	15	53%	0.09339995
Class 4_repressed	**11**	**15**	**73%**	**0.001996675**
Class 5_repressed	0	1	0%	N/A
Class 6_repressed	**6**	**8**	**75%**	**0.02081503**
Class 7_repressed	**13**	**18**	**72%**	**0.0009569**
TOTAL REPRESSED	**51**	**83**	**61%**	**2.10E-07**

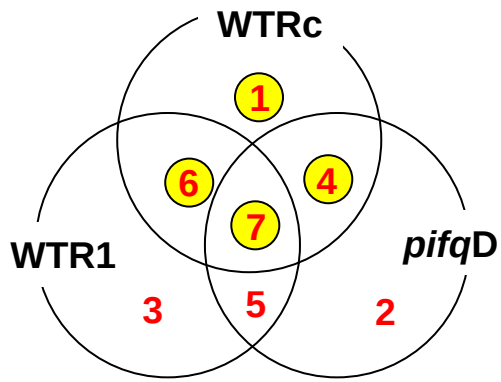

Supplemental Figure 10

Supplemental Figure 10. Statistical analysis for G-box enrichment in the 3Kbp-upstream putative promoter regions of SSTF genes by functional category.

A) Hypergeometric statistical test to asses the significance of G-box enrichment in the different SSTF genes by functional category compared to the total population of genes represented on the ATH1 array (Supplemental Figure 9A). Genes in the different induced and repressed functional groups are described in Figures 4 and 5. Functional groups highlighted in the table are the ones showing a statistically significant enrichment of genes with G-boxes (p-value ≤ 0.05).

B) Hypergeometric statistical test to asses the significance of G-box enrichment in each Class within the transcription factor functional group compared to the total population of genes represented on the ATH1 array (Supplemental Figure 9A). Transcription factors within the induced and repressed Class 1-7 genes are described in Figures 4 and 5. Highlighted Classes in the Venn diagram (right panel) are the ones showing a statistically significant enrichment of genes with G-boxes (p-value ≤ 0.05).

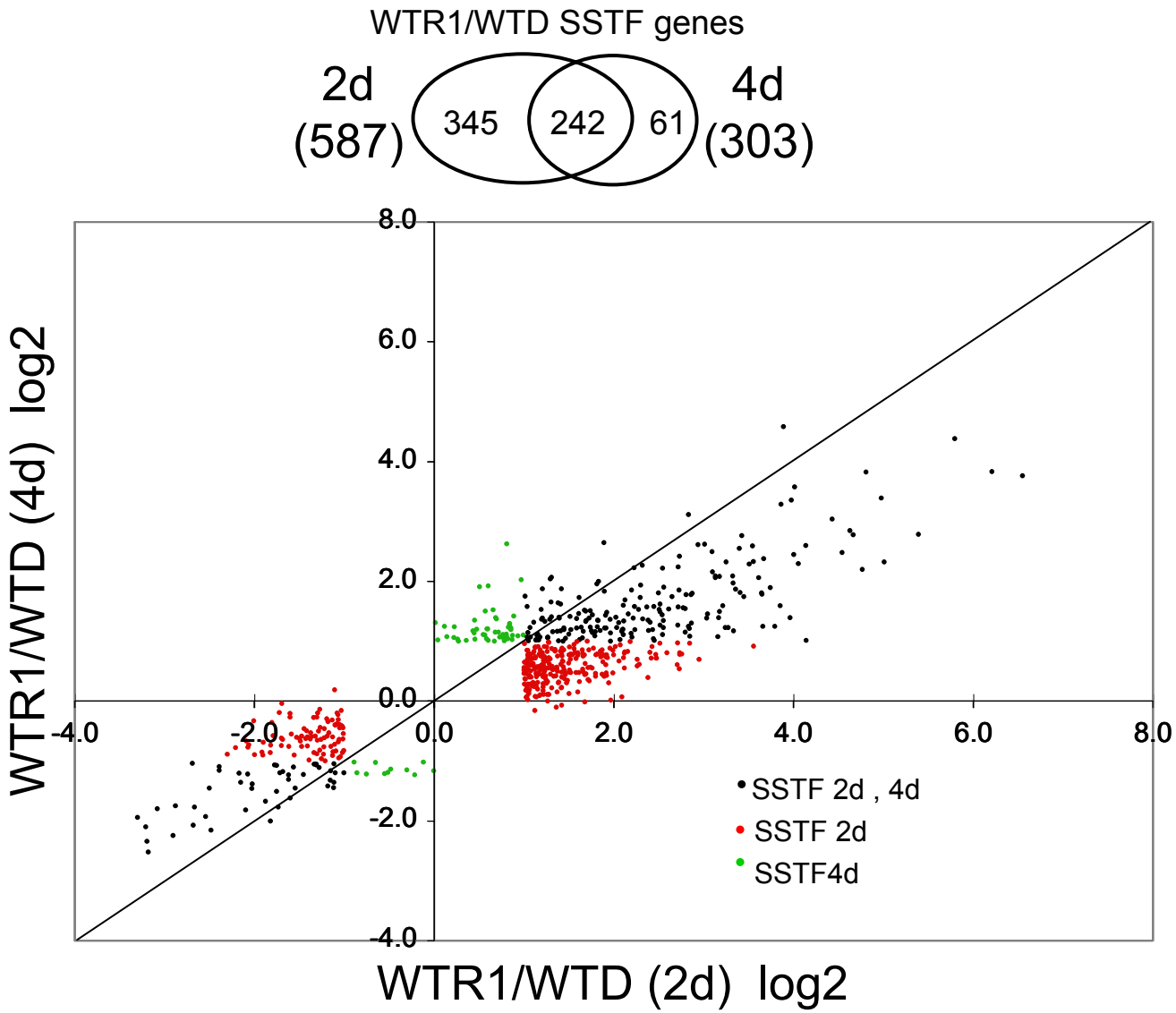

Supplemental Figure 11

Supplemental Figure 11. Comparison of 2d-old and 4d-old early-R1-responsive genes in wild-type seedlings.
(Top). Venn diagram shows pairwise comparison of SSTF genes responding to R1 (WT-R1 vs WT-D, Figure 3) in 2d-old and 4d-old seedlings. A list of SSTF genes reproducibly responding to R1 in 4d-old seedlings was obtained from multiple microarray experiments ((Monte et al., 2004; Tepperman et al., 2006); E. Kikis, J. Tepperman and P. Quail, unpublished). The list of genes within each of the 3 subgroups in the Venn diagram is included in Supplemental Dataset 6. (Bottom). Scatterplot of log2 fold-change values provide a quantitative measure of the responsiveness of each gene in the two different aged seedlings (2d vs 4d). Black dots in the scatterplot represent genes that are shared between the two comparisons in the Venn diagram (top) whereas red and green dots represent genes that are specifically present in one of the comparisons but not in the other.

PIF3 - dependent / light induced

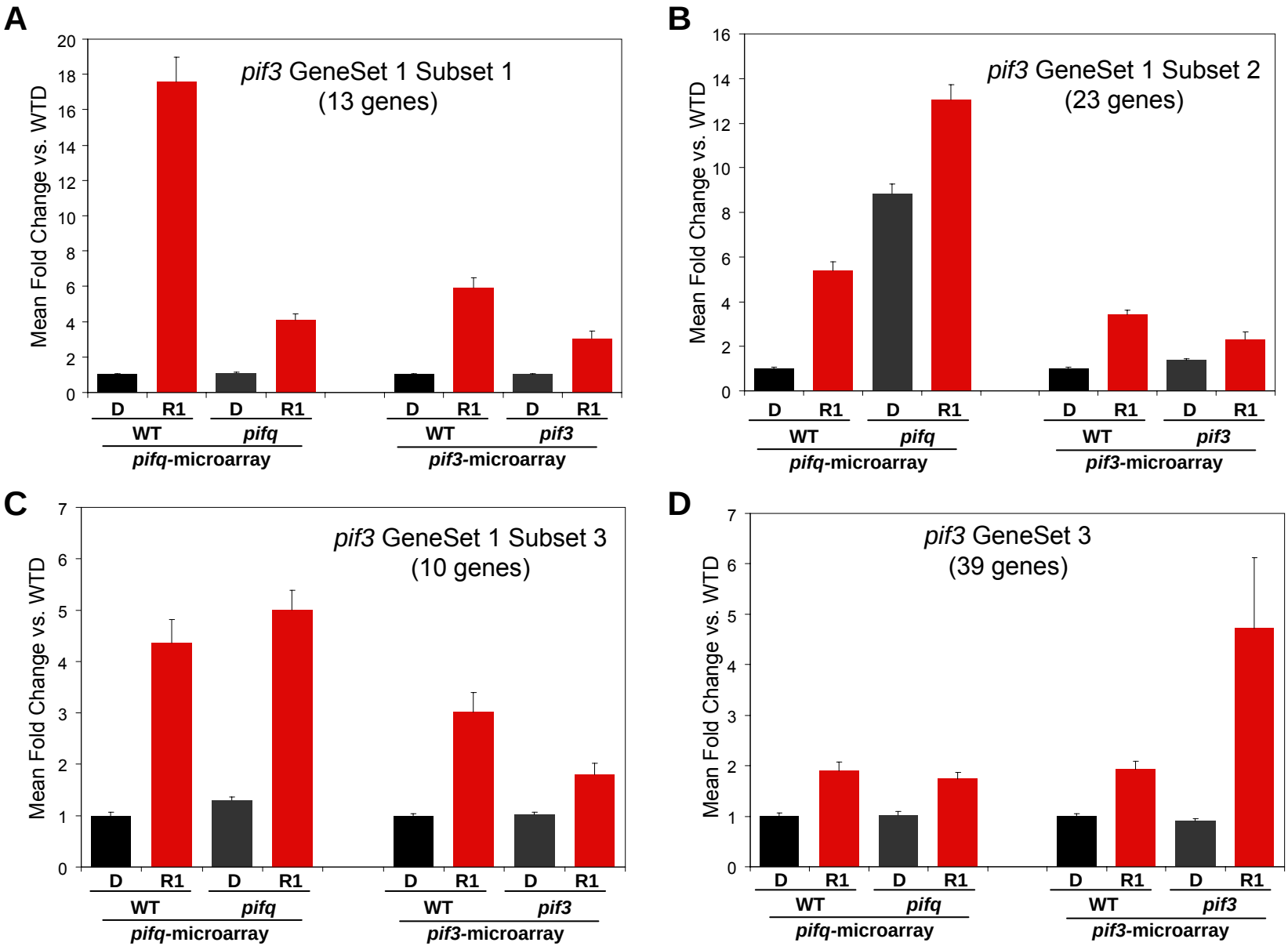

Supplemental Figure S12

Supplemental Figure 12. Comparative analysis of the expression profiles in the *pifq* (Supplemental Dataset 1) and *pif3* (Monte et al., 2004) mutants of genes defined as early-R1 induced that are PIF3-dependent for this R-light-induction.

The genes described as early-R1 induced that are PIF3-dependent for this R-light-induction (*pif3* Genesets 1 and 3; (Monte et al., 2004)) were divided into 4 subsets according to how they respond here in *pifq* mutant seedlings in the dark (panels A-D). Lists of genes corresponding to panels A-C are in Supplemental Dataset 7. The bar graphs in panels A-C represent the mean fold-change relative to WT-D. Error bars represent the mean standard error of the genes averaged in each subgroup. The data for the *pifq* microarray are from the present study (left) and for the *pif3* microarray are from (Monte et al., 2004) (right).

A) *pif3* GeneSet 1 - Subset 1 (13 genes). Genes that have similar expression profiles in the *pifq* and *pif3* mutants.

B) *pif3* GeneSet 1 - Subset 2 (23 genes). Genes that are SSTF (induced) in the *pifq*-D compared to WTD.

C) *pif3* GeneSet 1 - Subset 3 (10 genes). Genes that show no effect in the *pifq* mutant compared to WT.

D) *pif3* GeneSet 3 (37 genes). These genes were described as Rc-Induced genes displaying greater Rc-light-induced expression in the *pif3* mutant than in WT.

<u>Supplemental Figure 13.</u> Comparative analysis of the expression profiles in *pifq* (Supplemental Dataset 1) and *pif3* (Monte et al., 2004) mutants of genes described as early-R1 repressed that are PIF3-dependent for this R-light-repression.

The genes described as early-R1 repressed that are PIF3-dependent for this R-light-repression (Monte et al., 2004) were divided into 2 subsets according to how they respond here in the *pifq* mutant seedlings in the dark (panels A-B). Lists of genes corresponding to panels A-B are in Supplemental Dataset 7. The graphs in panels A-B represent the mean fold-change relative to WT-D. Error bars represent the mean standard error of the genes averaged in each subgroup.

A) Not SSTF genes in the *pifq*-microarray (3 genes). Genes that are not SSTF in *pifq*-D compared to WTD.

B) SSTF genes in the *pifq*-microarray (5 genes). Genes that are SSTF (repressed) in *pifq*-D compared to WTD.

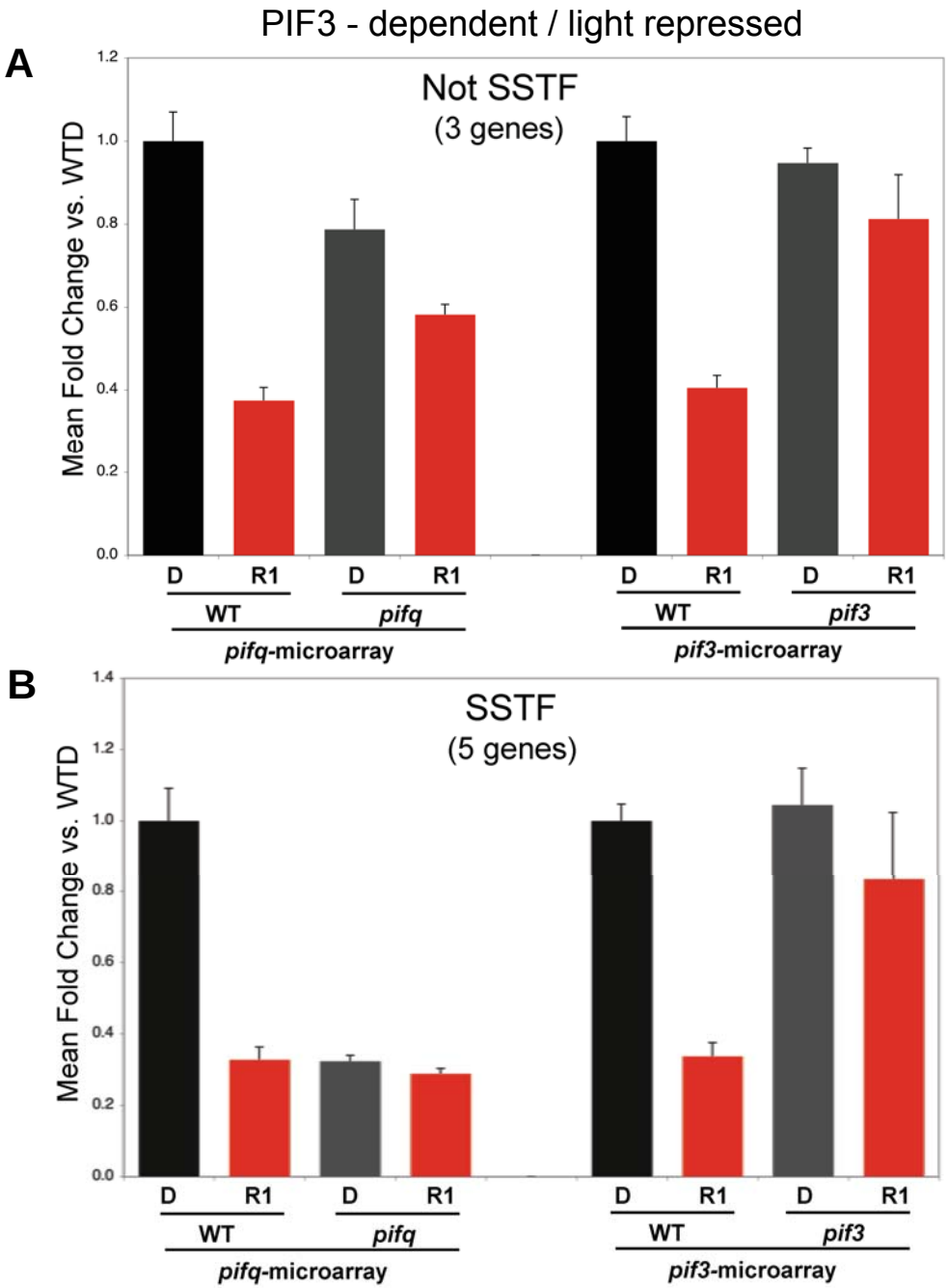

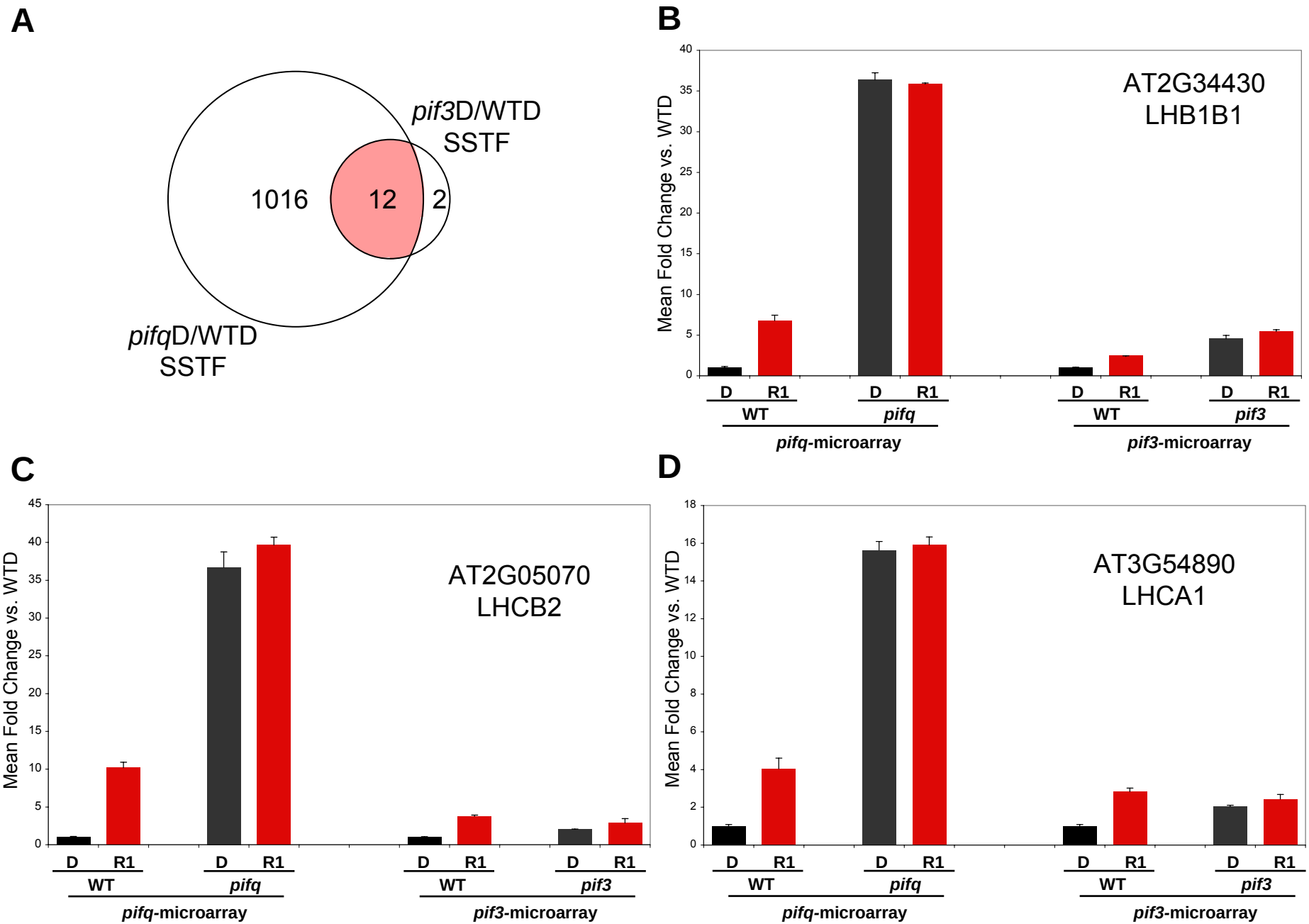

Supplemental Figure 14

Supplemental Figure 14. Comparative analysis of the expression profiles in *pifq* (Supplemental Dataset 1) and *pif3* (Monte et al., 2004) mutants of genes that are PIF3-regulated in the dark (WT-D vs *pif3*-D).
Differentially expressed SSTF genes in the *pif3* mutant in the dark compared to WT were defined using the published data (Monte et al., 2004). Lists of the genes in Panel A are in Supplemental Dataset 8. Venn diagram in panel A shows pairwise comparison of SSTF genes responding to *pif3*-D in 4d-old seedlings (WT-D vs *pif3*-D, (Monte et al., 2004)) and to *pifq*-D in 2d-old seedlings (WT-D vs *pifq*-D, Figure 3). Individual profiles of genes responding in SSTF fashion to both 1h of Rc in WT and in the *pif3* mutant in darkness are shown in panels B-D. Data represent mean expression values relative to dark-grown wild-type (WT-D) set as a unity, and bars represent standard error of at least three biological replicates.

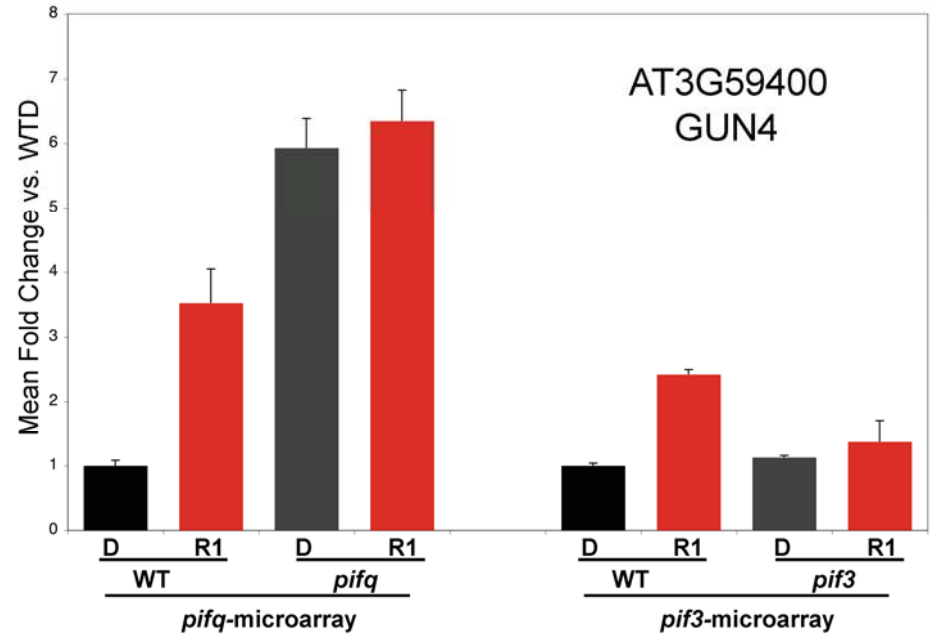

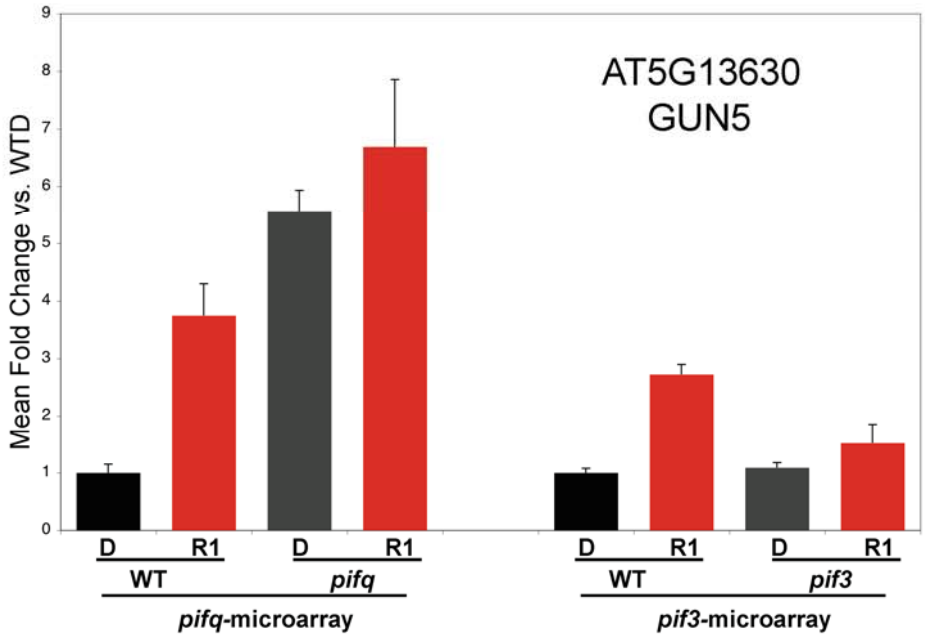

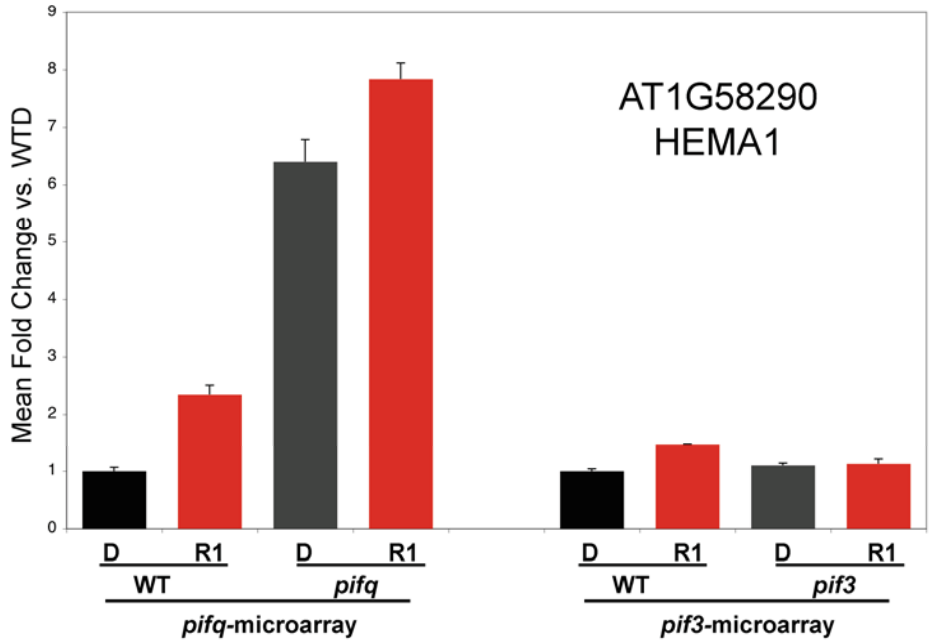

<u>Supplemental Figure 15.</u> Comparative analysis of the expression profiles in the *pifq* (Supplemental Dataset 1) and *pif3* (Monte et al., 2004) mutants of PIF3-regulated tetrapyrrole biosynthesis genes reported by (Stephenson et al., 2009).

The *pif3* microarray data are from (Monte et al., 2004), and the *pifq* microarray data are from the present study. Data represent mean expression values relative to dark-grown wild-type (WT-D) set as a unity, and bars represent standard error of at least three biological replicates.

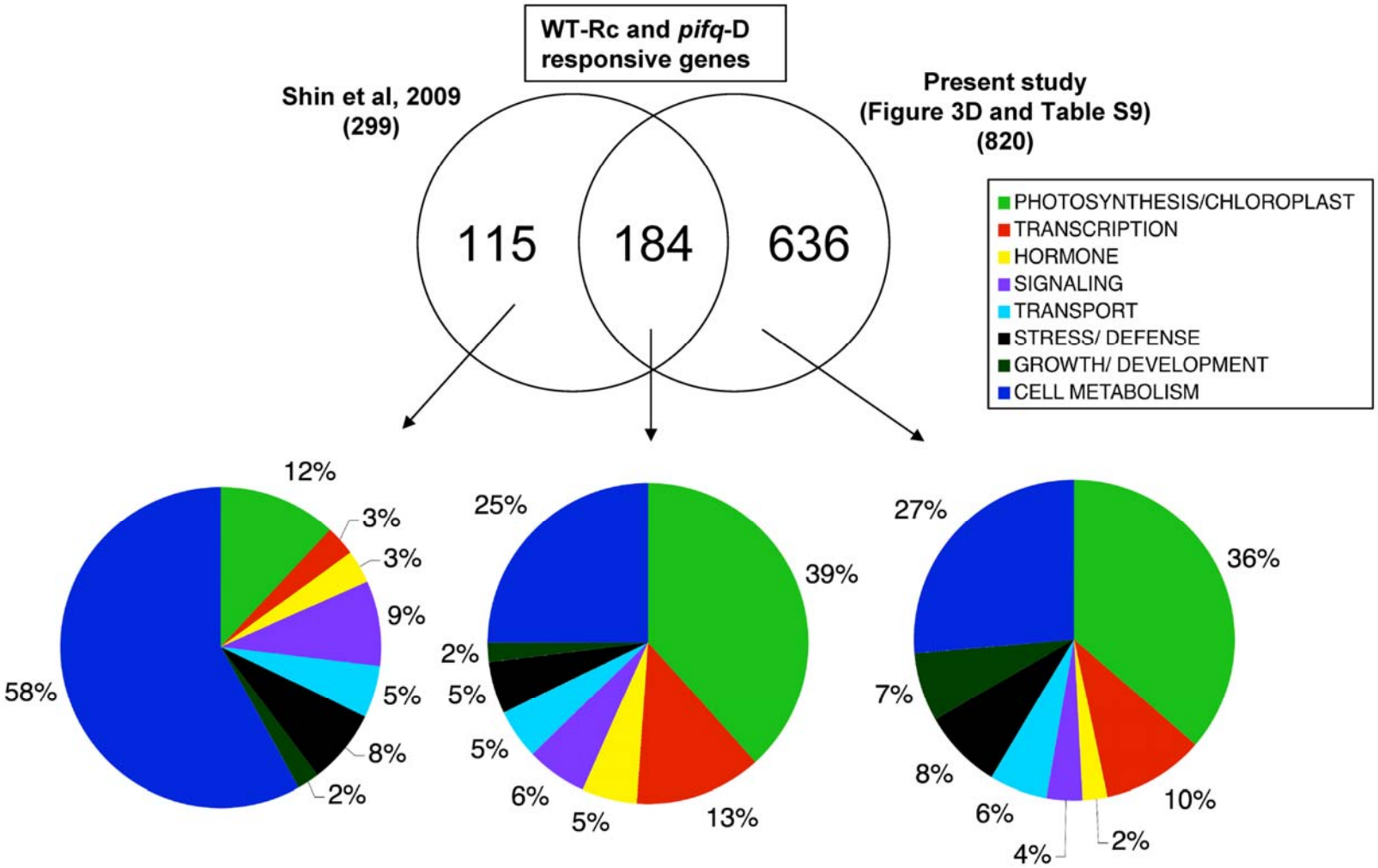

<u>Supplemental Figure 16.</u> Comparison of SSTF genes described as responsive to both WT-Rc and *pifq*-D compared to WT-D in this study (Figure 3D and Supplemental Dataset 1) and in (Shin et al., 2009).

Venn diagram (top) shows pairwise comparison of the 820 SSTF genes responding to both WT-Rc and *pifq*-D in the present study (Figure 3D, top) and in (Shin et al., 2009). For this comparison, 299 genes (out of 332) reported by Shin et al. represented on the ATH1 array were used. Supplemental Dataset 9 contains the list of genes reported by Shin et al. that are absent in ATH1 array, as well as the genes falling into each subgroup of the Venn diagram. The distribution of genes in each subgroup of the Venn diagram among functional categories is shown as the percentage of the total annotated genes within each bin for each subgroup (bottom). Functional categories were established as in Figure 5.

Supplemental Table 1. **Primer sequences used for q-PCR.**

		Forward Primer (5' to 3')		Reverse Primer (5' to 3')	Reference
PP2A – AT1G13320	**PLR74**	TAT CGG ATG ACG ATT CTT CGT GCA G	**PLR75**	GCT TGG TCG ACT ATC GGA ATG AGA G	**Shin et al, 2007**
ELIP2 - AT4G14690	**CMM102**	GGC AGA GGC AAA GTC AAA AGG	**CMM103**	CGC AAC GAG ACC GAG CAT	
CCA1 - AT2G46830	**CMM192**	CCG CAA CTT TCG CCT CAT	**CMM193**	GCC AGA TTC GGA GGT GAG TTC	
GUN5 - AT5G13630	**CMM106**	GGC TGG ACG CAA GAA CAA AG	**CMM107**	GCA CTC CAT CCC ACA GTG TTG	
COL2 - AT3G02380	**CMM204**	CCA CGG ATC AAG GGC AGA T	**CMM205**	GGA AGG GAC AAT TCC ATA TCC A	
LHB1B1-AT2G34430	**PLR84**	CGT CCC CGG AAA GTG AGT T	**PLR85**	TGC AAC AAA CCG GAT ACA CAC	**Leivar et al, 2008b**
PIL1 - AT2G46970	**PLR90**	AAA TTG CTC TCA GCC ATT CGT GG	**PLR91**	TTC TAA GTT TGA GGC GGA CGC AG	**Salter et al, 2003**
HAT4/ATHB2 - AT4G16780	**CMM186**	GTC GTT GCC GGT CAA TGC	**CMM187**	CCT AGG ACG AAG AGC GTC AAA A	
AUX/IAA29 - AT4G32280	**CMM134**	CAC CAT CAT TGC CCG TAT CA	**CMM135**	CCA CAG TAG CCG TTG TTG GA	
SAUR2 - AT4G13790	**CMM252**	CGG AAT CAT TAT CAA CGC CTA AA	**CMM253**	TGT TCA AGT AAC AAA CCG GAA CA	
Unknown-AT5G02580	**CMM182**	CAT CCA TTT GGT GCA TCA TTT G	**CMM183**	CAC TCT TCT TTG CCC ATG TTG A	

SUPPLEMENTAL ANALYSIS 1. Promoter analysis for potential PIF-protein target sites

Computational analysis of the 3kb region upstream of the transcription start sites of the genes identified in the transcriptome analysis shows that the frequency of G-box containing promoters in the different gene Classes ranges from 37 to 78% of the induced genes, and from 37 to 59% for the repressed genes (excluding the single gene in Class 5) (Figure 4 and Supplemental Figure 9). Interrogation of the TAIR database (http://www.arabidopsis.org/cgi-bin/patmatch/nph-patmatch.pl) indicates that, on average genome-wide, 34% of Arabidopsis 3kbp upstream promoter regions of the genes represented on the ATH1 array contain one or more G-box motifs (Supplemental Figure 9A). Hypergeometric-distribution analysis of these data indicates that several of the gene Classes exhibiting high percentages of genes containing G-box motifs in their promoter regions are statistically significantly enriched for this motif, relative to this genome-wide average level. These are Classes 1 (39%), 3 (53%), 5 (78%), and 7 (48%) of the induced genes and Classes 3 (49%), 4 (50%) and 7 (59%) of the repressed genes (Supplemental Figure 9B), consistent with possible direct PIF regulation of at least some of those genes.

Statistically significant promoter G-box enrichment is also apparent within certain functionally-defined categories both across (Supplemental Figure 10A) and within (Supplemental Figure 10B) certain gene Classes. Photosynthesis/Chloroplast(P/C)- and transcription-related genes are prominent in this respect. The transcription-related genes are particularly notable in this regard, where 60% of the induced Class 3 gene promoters contain G-boxes, and 56%, 73%, 75% and 72% of the repressed Class 1, 4, 6 and 7 gene promoters contain G-boxes, respectively (Supplemental Figure 10B). Because the Class 3, 6 and 7 genes are rapidly light-responsive, the G-box-containing members of these Classes are candidates for direct PIF regulation. However, because the Class 1 and 4 genes exhibit delayed responsiveness to light, the probability increases that they may instead be indirect targets. Intriguingly, in addition, it is notable that the statistically-significant G-box enrichment in the induced transcription-related genes is confined to the rapidly but transiently light-induced Class 3 genes, whereas enrichment in the repressed transcription-related genes is present in all four Classes (1, 4, 6 and 7) that exhibit sustained repression in response to Rc (WT-Rc)(Supplemental Figure 10). This might be

consistent with a different mode of action of the PIF proteins in regulating these light-induced and light-repressed genes. Also notable, is the absence of G-box enrichment in the Class 2 genes. This might indicate longer-term indirect regulation by the PIFs of these non-light responsive genes.

SUPPLEMENTAL ANALYSIS 2. Comparative expression analysis

To begin to gain preliminary insight into the possible contribution of the individual PIF proteins to the collective action of the four PIFs on gene expression documented here, we compared the expression patterns of the *pifq* mutant with those previously reported for the monogenic *pif3* mutant (Monte et al., 2004) in response to 1h of R. Although this comparison suffers from the shortcoming that it compares seedlings of different age and growth history (*pif3* was grown under "pseudo-dark" conditions for 4 d in the dark before R1 irradiation, compared to *pifq* grown here under "true-dark" conditions for only 2 d before R1 irradiation), the data appear to be informative in three respects. First, comparison of the responsiveness of WT 2-d and 4-d dark-grown seedlings to 1 h of R shows a qualitatively similar, albeit quantitatively different pattern. Of the 303 SSTF light-regulated, early-response genes reproducibly detected in WT 4d-seedlings over multiple experiments ("consensus" early-response genes) ((Monte et al., 2004; Tepperman et al., 2006); E. Kikis, J. Tepperman and P. Quail, unpublished), 80% (242 genes) also display SSTF responsiveness to 1 h R in the 2d-seedlings (Supplemental Figure 11 and Supplemental Dataset 6). However, as shown in the scatter plot in Supplemental Figure 11, the magnitude of the expression-response to the R1 signal is apparently substantially greater for most genes in the 2d- than the 4d-seedlings, such that almost twice as many genes (587) reach the SSTF threshold in the 2d- than the 4d-seedlings.

Second, of the 46 induced, early-response genes previously identified in the 4d seedlings as dependent on PIF3 for rapid R1-induction (GeneSet 1; (Monte et al., 2004)), 13 genes (28%, designated as Subset 1 here) retain the same pattern of expression in the 2d seedlings (Supplemental Figure 12A and Supplemental Dataset 7), namely a requirement for the PIFs for rapid R1 induction, without evidence of these factors having any SSTF effect on expression in the dark. Included in this Subset 1 are *ELIP1, SIGE* and

CPA-FA SYNTHASE (AT3G23530). On the other hand, 23 genes (50%) (designated Subset 2 here), display a robust SSTF induction in the 2d dark-grown *pifq* controls, that was absent (for most genes) or weak (for three genes) in the *pif3* mutant at 4d (Supplemental Figure 12B and Supplemental Dataset 7). These data thus reproduce the original PIF3-dependent, early-response induction for one subset (Supplemental Figure 12A), but uncover a previously undetected constitutive PIF-activity for another subset (Supplemental Figure 12B), suggesting a possible dichotomy in PIF regulation of these two subsets of genes. The remaining 22% of genes in the original GeneSet 1 (10 genes, designated Subset 3 here) displayed no significant dependence on the four PIFs for expression either in the dark or light in the 2d seedlings in the present study (Supplemental Figure 12C and Supplemental Dataset 7), thus failing to reproduce the previously observed PIF3 dependence. Similarly, of 39 R1-induced genes originally identified as displaying converse hypersensitivity to the light signal in the 4d *pif3*-mutant seedlings (GeneSet 3; (Monte et al., 2004)), none display reproducibility of this hypersensitive response to the absence of the PIFs in the 2d *pifq* mutant here (with one exception, *CP1* AT5G49480) (Supplemental Figure 12D and Supplemental Dataset 7). As a high proportion of the GeneSet 3 genes are stress-related (Monte et al., 2004), it is possible that the original expression-hypersensitivity observed for 4d-*pif3* seedlings reflected the subsequently-noted partial photobleaching of these older seedlings ((Shin et al., 2009; Stephenson et al., 2009); Supplemental Figure 2). Of the 8 repressed, early-response genes previously identified in the 4d seedlings as dependent on PIF3 for rapid R1-repression (Monte et al., 2004), 3 genes display a similar PIF-dependence for light-responsiveness in the *pifq* mutant in the 2d seedlings here (Supplemental Figure 13A and Supplemental Dataset 7). On the other hand, the remaining 5 genes display constitutive reduction of expression in the dark in the 2d *pifq*-mutant seedlings in the present study (Supplemental Figure 13B and Supplemental Dataset 7).

Third, not presented in our previous study on PIF3-dependent gene expression (Monte et al., 2004) were the changes in expression in the 4d dark-grown *pif3* monogenic mutant compared to the similarly dark-grown WT seedlings. Those data are compared here now with those for the 2d dark-grown *pifq* mutant in the present study. A total of only 14 genes (7 induced and 7 repressed) were found to differ in SSTF fashion in the

dark-grown *pif3* mutant (*pif3*-D) relative to the level of expression in the dark-grown WT control. This result is in stark contrast to the total of 1028 Class 2, 4, 5 and 7 genes identified here as differing in SSTF fashion between dark-grown *pifq* (*pifq*-D) and WT (WT-D) seedlings (Figure 3B). Twelve of the 14 *pif3*-D genes (7 induced and 5 repressed) overlap with those of the *pifq*-D genes (Supplemental Figure 14A and Supplemental Dataset 8). However, 9 of these 12 genes were not SSTF early-response genes (WT-D vs WT-R1 comparison) in the *pif3* experiment and, therefore, were not investigated for PIF3 involvement. The remaining 3 genes (*LHB1B1* (AT2G34430), *LHCB2.2* (At2G05070) and *LHCA1* (At3G54890)) do display induction in both *pif3* and *pifq* dark-grown mutants, but this response is substantially more robust in the *pifq* mutant, where they are Class 7 induced genes (Supplemental Figure 14B-D).

Taken together, these data suggest that the absence of PIF3 alone in the monogenic *pif3* mutant has minimal detectable effect on gene expression in dark-grown seedlings compared to *pifq*, but has a relatively quantitatively weak effect in reducing the magnitude of the rapid light-induced expression of a small subset of genes (Supplemental Figures 12-14). A similarly minimal effect was reported for the absence of PIF1 alone in a microarray analysis of a monogenic *pif1* mutant, where the expression of only three genes was altered reproducibly in SSTF fashion between the 4-d dark-grown mutant and WT (Moon et al., 2008). Another recent report examined the expression of three chlorophyll-biosynthesis genes, *HEMA1, GUN4* and *CHLH* (*GUN5*), in dark-grown *pif1* and *pif3* monogenic, and *pif1pif3* double mutants using qPCR analysis (Stephenson et al., 2009). These authors reported the absence of two-fold changes in expression of these genes in 4-d dark-grown seedlings of all three mutants, confirming our earlier observations for the *pif3* monogenic mutant (Supplemental Figure 15; (Monte et al., 2004)). They did, however, report two-fold or greater enhancement of expression of these genes in 2-d and/or 3-d dark-grown seedlings of these mutants, with some evidence that the double mutant has an additive phenotype compared to the two monogenic mutants. Our present data are consistent with these, showing strong derepression of expression of all three genes in the dark-grown *pifq* mutant (Supplemental Figure 15).

Direct comparison of comparable aspects of our present data with those in a recent study by (Shin et al., 2009), highlights some interesting contrasts. These authors

also examined the differential gene expression between WT seedlings grown in continuous R and a *pifq* mutant grown in darkness. Strikingly, only 22% of the genes that we identified as being expressed in common, in SSTF fashion, between WT and mutant (Classes 4 and 7 combined) overlap with those identified by Shin et al. (Supplemental Figure 16; Supplemental Dataset 9). This is partly because we identified a higher number of common genes than these authors, but in addition, over one-third of the genes in the Shin et al. study do not coincide with ours. Examination of the distributions of the functional categories of genes between the three sectors of the Venn diagram in Supplemental Figure 16 shows that the pattern inherent in our combined Class 4 and 7 genes is remarkably conserved in both the subset that overlaps (central sector), and that which does not (right-hand sector), with the Shin et al. gene-set. This pattern indicates strong enrichment for chloroplast/photosynthesis- and transcription-factor-genes, consistent with a function in the deetiolated state of the seedling (Figure 5). By contrast the non-overlapping subset of Shin et al. genes (left-hand sector) displays a substantially different pattern, markedly depleted in these two gene categories and strongly enriched in cell-metabolism genes (Supplemental Figure 16). Possible reasons for these differences are discussed in the Discussion.

SUPPLEMENTAL METHOD 1. Light and Transmission Electron Microscopy (TEM)

Cotyledons from 2d-old dark- and Rc-grown seedlings were fixed in 8% glutaraldehyde in a 0.05M sodium cacodylate buffer pH 7.2 at 4ºC for several days. High pressure freezing and microwave processing methods were used for sample preparation. For the high pressure freezing (HPF) method, fixed samples were frozen in an EM PACT2-RTS high pressure freezing machine (Leica Microsystems, Vienna, Austria) as follows: a single cotyledon was placed in a 100 micrometer deep “membrane carrier” and the remaining space was filled with a thick paste made up of dried yeast cells mixed with 8 percent methanol (McDonald et al., 2007). The carrier was loaded into the EM PACT2 Rapid Transfer System loading device and inserted into the HPF machine where it was frozen within milliseconds at 2050 bars pressure and at a cooling rate of approximately 27,000 ˚K/s. Frozen cells were processed in an automated freeze substitution device

(Leica Microsystems, Vienna, Austria) over a period of 3 days (22 hours at -90˚C, warmed to -25˚C at 2˚C per hour, left at -25˚C for 12 hours, warmed to 20˚C at 5˚C/hour). The freeze substitution fixative consisted of 1% osmium tetroxide (OsO_4) plus 0.1% uranyl acetate in acetone. Samples were rinsed in three changes of pure acetone, then infiltrated in 25% increments in Epon-Spurr's resin (McDonald and Muller-Reichert, 2002) over 2 days. Cotyledons were oriented in latex flat embedding molds and polymerized for 2 days at 60˚C. 70 nm thin sections were collected on mesh or slot grids, stained for 7 min each in 2% uranyl acetate and lead citrate, and observed in a Tecnai 12 transmission electron microscope operating at 100kV. Images were recorded with a Gatan Ultrascan 1000 CCD camera.

For microwave (MW) processing, the fixed cotyledons were processed in a Pelco Model 3440 Laboratory Microwave with Coldspot® and variable wattage controller (Ted Pella, Inc., Redding, CA) as follows: after three rinses with buffer (0.1M sodium cacodylate, pH 7.2), whole seedlings were post-fixed in 1% OsO_4 plus 0.8% potassium ferricyanide in buffer for one minute, then pulsed for 40 sec at 150W in the MW, followed by another minute in the fixative without microwave power. This step was repeated once. Following 2 rinses in dH2O of 40 sec each in the MW at 150 W, dehydration was accomplished by two 40 second rinses in the MW (150 W) at each step of 10, 20, 30, 50, 70, 90, 95, 100, and 100% acetone. Resin infiltration was in 2 steps each of 25, 50, 75 and 100% acetone:resin mixtures with MW irradiation at 250 W for 3 min in 20 mm Hg vacuum. Resin polymerization, sectioning and microscope observations were as above.

Prolamellar body (PLB) area as a % of host-etioplast area and mean prothylakoid length per etioplast were quantified in a manner similar to Wellburn et al. (Wellburn et al., 1983). Image J was used to measure those parameters from at least 76 etioplasts from several different TEM micrographs.

For light microscopy examination, resin sections 0.5 □m thick were taken from the same blocks used for TEM observations (microwave method), dried down on a microscope slide by heating on a slide warmer, stained with 1% toluidine blue plus 1% sodium borate, and heated again for about 1 minute on a slide warmer. Slides/sections were rinsed with water and allowed to dry before observation with a light microscope.

SUPPLEMENTAL REFERENCES

Leivar, P., Monte, E., Al-Sady, B., Carle, C., Storer, A., Alonso, J.M., Ecker, J.R., and Quail, P.H. (2008a). The Arabidopsis phytochrome-interacting factor PIF7, together with PIF3 and PIF4, regulates responses to prolonged red light by modulating phyB levels. Plant Cell **20,** 337-352.

Leivar, P., Monte, E., Oka, Y., Liu, T., Carle, C., Castillon, A., Huq, E., and Quail, P.H. (2008b). Multiple phytochrome-interacting bHLH transcription factors repress premature seedling photomorphogenesis in darkness. Curr Biol **18,** 1815-1823.

McDonald, K., and Muller-Reichert, T. (2002). Cryomethods for thin section electron microscopy. Methods Enzymol **351,** 96-123.

McDonald, K.L., Morphew, M., Verkade, P., and Muller-Reichert, T. (2007). Recent advances in high-pressure freezing: equipment- and specimen-loading methods. Methods Mol Biol **369,** 143-173.

Monte, E., Tepperman, J.M., Al-Sady, B., Kaczorowski, K.A., Alonso, J.M., Ecker, J.R., Li, X., Zhang, Y., and Quail, P.H. (2004). The phytochrome-interacting transcription factor, PIF3, acts early, selectively, and positively in light-induced chloroplast development. Proc Natl Acad Sci U S A **101,** 16091-16098.

Moon, J., Zhu, L., Shen, H., and Huq, E. (2008). PIF1 directly and indirectly regulates chlorophyll biosynthesis to optimize the greening process in Arabidopsis. Proc Natl Acad Sci U S A **105,** 9433-9438.

Salter, M.G., Franklin, K.A., and Whitelam, G.C. (2003). Gating of the rapid shade-avoidance response by the circadian clock in plants. Nature **426,** 680-683.

Shin, J., Park, E., and Choi, G. (2007). PIF3 regulates anthocyanin biosynthesis in an HY5-dependent manner with both factors directly binding anthocyanin biosynthetic gene promoters in Arabidopsis. Plant J **49,** 981-994.

Shin, J., Kim, K., Kang, H., Zulfugarov, I.S., Bae, G., Lee, C.H., Lee, D., and Choi, G. (2009). Phytochromes promote seedling light responses by inhibiting four negatively-acting phytochrome-interacting factors. Proc Natl Acad Sci U S A **106,** 7660-7665.

Stephenson, P.G., Fankhauser, C., and Terry, M.J. (2009). PIF3 is a repressor of chloroplast development. Proc Natl Acad Sci U S A **106,** 7654-7659.

Sturn, A., Quackenbush, J., and Trajanoski, Z. (2002). Genesis: cluster analysis of microarray data. Bioinformatics **18,** 207-208.

Tepperman, J.M., Hwang, Y.S., and Quail, P.H. (2006). phyA dominates in transduction of red-light signals to rapidly responding genes at the initiation of Arabidopsis seedling de-etiolation. Plant J **48,** 728-742.

Wellburn, A.R., Gounaris, I., Fäßler, L., and Lichtenlhaler, H.K. (1983). Changes in plastid ultrastructure and fluctuations of cellular isoprenoid and carbohydrate compounds during continued etiolation of dark-grown oat seedlings. Physiol Plant **59,** 347-354.